MISS MARÍA HELENA RAMÍREZ ACOSTA (Orcid ID : 0000-0001-6023-1693)

DR DANIEL ROBERTO CASSAR (Orcid ID : 0000-0001-6472-2780)

DR MAZIAR MONTAZERIAN (Orcid ID : 0000-0002-1409-9182)

DR EDGAR DUTRA ZANOTTO (Orcid ID : 0000-0003-4931-4505)

Article type : Original Article

Further evidence against the alleged failure of the classical nucleation theory below the glass transition range

María Helena Ramírez Acosta[1], Lorena Raphael Rodrigues, Daniel Roberto Cassar, Maziar Montazerian, Oscar Peitl Filho, Edgar Dutra Zanotto

Graduate Program in Materials Science and Engineering, Department of Materials Engineering, Federal University of São Carlos, São Carlos, Brazil

Abstract

We collected a plethora of *new* data to test the hypothesis that the failure of the Classical Nucleation Theory (CNT) below the glass transition range is just an experimental artifact. Since reaching the steady-state nucleation regime takes a significant time for treatments below the glass transition temperature, data collected in this temperature range tend *not* to have reached a steady-state. Because of this potential problem, we examined the CNT using *new* experimental data for

[1] E-mail: churimahe@hotmail.com

This article has been accepted for publication and undergone full peer review but has not been through the copyediting, typesetting, pagination and proofreading process, which may lead to differences between this version and the Version of Record. Please cite this article as doi: 10.1111/JACE.17852

three stoichiometric silicate glasses: $Li_2Si_2O_5$, $BaSi_2O_5$, and $Na_4CaSi_3O_9$. We also measured the equilibrium viscosity for the studied glass batches and used it as a proxy for the effective diffusion coefficient. The analysis was conducted by applying a steady-state criterion and evaluating the error propagation throughout all calculations. Using this rigorous procedure, we have *not* observed the alleged CNT failure. Our comprehensive results support recent studies questioning this possible CNT failure helping solve a longstanding problem in glass science.

Keywords: glass**;** crystallization; viscosity; classical nucleation theory; silicate.

1 Introduction

Knowledge of the mechanism and kinetics of crystal nucleation in glass-forming liquids has significant technological and scientific importance, encompassing the development of stable glass compositions, the design of novel glass-ceramics, and the formulation and improvement of theories to explain and predict crystallization kinetics.

A varied toolset of methods is available for describing and predicting nucleation kinetics, such as the Classical Nucleation Theory (CNT), the Diffuse Interface Theory (DIT), and the Density Functional Theory (1). Among them, the CNT is the most widely used to evaluate nucleation rates of a new phase (2). Nevertheless, this theory has some limitations, which need to be settled to validate its descriptive and predictive power. The first failure observed in CNT is the considerable underestimation in describing the experimental steady-state nucleation rates (J_0) when a fitted, average value of the nucleus/liquid interfacial energy (σ) is used (3,4). However, this problem can be eliminated by force-fitting a temperature-dependent interfacial energy, $\sigma(T)$ (5,6), which is predicted by the DIT.

Another limitation of the CNT is the alleged inability in describing the temperature dependence of J_0 below the maximum nucleation temperature (T_{max}), which is usually close to the glass transition temperature (T_g) for oxide glass-formers (7). This apparent failure, known as "CNT breakdown" or "CNT anomaly", has been reported by different researchers throughout the past 40 years (6,8–11). As a consequence, several hypotheses have been raised aiming to explain its origin. For example, errors due to the replacement of the effective diffusion coefficient for nucleation (D_J) by the inverse of the shear viscosity (η) (8), the possibility of metastable phase formation during the early stages of the nucleation (12), the effect of elastic strain on the free energy of critical nucleus formation (13), a possible (unexpected) steep variation of the size of the

"structural units" at temperatures below T_g (9), and the influence of dynamic heterogeneities in the critical nucleus size (14). According to these studies, metastable phase formation, evaluation of D_J by the inverse of η, and the effect of elastic strain cannot explain the "CNT breakdown". Besides that, the other explanations, albeit feasible, are limited to theoretical analyses, without experimental verification so far.

Therefore, despite the numerous efforts to understand this problem, it remains some open questions. Hence, some groups (including ours) have decided to consider another possible explanation relating to an aspect commonly overlooked by most research. This alternative is associated to the lack of nucleation data obtained by very long heat treatments at temperatures below T_g, at which the time required to reach a steady-state condition is much longer than that typically used in experimental determinations of nucleation rates (11,15,16). The first attempt to test this new hypothesis ascribing the hypothetical failure of CNT to an experimental artifact was presented by one of us, Edgar D. Zanotto, at the American Ceramic Society´s GOMD 2018, in San Antonio, USA (17); then by Daniel R. Cassar at the International Congress on Glass, in Boston 2019, USA (18) and in poster form by María Helena R. Acosta in the same meeting (19). As a result of these presentations, a preprint was deposited in ArXiv (2019) (20), which finally resulted in a full paper published in 2020 (15).

In ref. (15), the hypothesis that the breakdown is just a byproduct of nucleation datasets that have *not* reached the steady-state regime was rigorously tested. The authors analyzed published nucleation data for 4 oxide supercooled glass-formers, $Li_2Si_2O_5$, $Na_2Ca_2Si_3O_9$, $Na_4CaSi_3O_9$, and $Ba_2TiSi_2O_8$, using only nucleation rates and viscosity data measured in samples of the same glass batch that satisfied a steady-state regime test. Furthermore, all the uncertainty and regression confidence bands were computed and considered. Having this rigorous protocol, among the 6 datasets analyzed, they only found weak evidence for which the existence of the nucleation break in 2 of them could not be discarded. Thus, their collective results indicate that if this break at T_{max} exists, it is *not* a common feature of all glass-formers.

Similarly, Xia et al. deposited an ArXiv manuscript (2020) (21) with experimental results for a barium silicate glass demonstrating that the anomaly at T_{max} arises from insufficient annealing times at low temperatures. In the resulting article, which was recently published (16), they measured the time-dependent nucleation rate in a $Ba_5Si_8O_{21}$ glass at a temperature 50 K below T_{max} for a very long time (115 days) and obtained results consistent with the predictions of the CNT, with no break at T_{max}. Since the breakdown has been reported for different silicate glasses,

the authors concluded that much of the existing nucleation rate data at low temperatures have not reached a steady-state regime. Despite these important findings, a definitive rejection of the existence of the "CNT breakdown" remained uncertain because in (15) it was not possible to discard it in two glasses, probably due to the use of literature data, whereas in (16) only one glass was tested at a single temperature below T_{max}.

In addition to those two papers, new publications have arisen, drawing attention to the generalized assumption in applying CNT and other theoretical crystallization models that nucleation proceeds only after the glass has completed the structural relaxation process towards the metastable supercooled liquid (SCL) state. In this regard, Schmelzer et al. (22) proposed a new hypothesis and provided a *theoretical* treatment of a different situation when nucleation proceeds *concomitantly* with structural relaxation. Such theoretical model is significant for the present work, since it offers a plausible explanation to the very long times required before nucleation reaches a steady-state, as reported in refs. (15) and (16).

The hypothesis and model proposed in (22) were tested by Fokin et al. (23), using a lithium disilicate glass as a model glass-forming substance. In therein nucleation *experiments* were carried out for very extended times (up to about 2,200 hours), at temperatures ~20 K below the laboratory T_g. Their results show that crystal nucleation starts *simultaneously* with glass relaxation towards the SCL, which strongly affects the nucleation kinetics, taking over 500 hours to reach the ultimate steady-state regime at this temperature. Such a long time is due to the decreasing in the work of critical nucleus formation, assigned to structural relaxation process, leading to a continuous increase of the nucleation rate. On the whole, the theoretical model proposed in (22) and the experimental results and analyses presented in (23) prove the effect of glass relaxation on crystal nucleation, and confirm the results of Cassar et al. (15) and Xia et al. (16) that the alleged "breakdown" of the CNT at temperatures close and below T_g results from the improper use of non-steady-state nucleation rates.

In view of these important findings and knowing that only a few glasses have been rigorously tested so far for this possible break, the main objective of this work is to *extend* the analysis of the steady-state versus the non-steady state hypothesis of the low-temperature CNT breakdown, considering our *new* extensive experimental dataset for low temperatures for three stoichiometric glasses, $Li_2Si_2O_5$, $BaSi_2O_5$ and $Na_4CaSi_3O_9$, which undergo internal homogeneous nucleation in laboratory time scales. The protocol for this work includes: i) using nucleation and viscosity data obtained at sufficiently low temperatures from samples of the same glass batches, ii) applying a

criterion to establish if steady-state nucleation was (likely) reached, and iii) consideration of error propagation throughout all the calculations and analysis.

2 Theoretical Framework

2.1 *Classical Nucleation Theory*

The formulation of the CNT is based on the thermodynamic description of heterogeneous systems developed by Gibbs (24), where a non-homogeneous system is substituted by a model system consisting of two homogeneous phases divided by a mathematical surface of negligible thickness. According to the CNT and commonly used assumptions, the temperature dependence of the steady-state nucleation rate ($J_0(T)$) can be described by Eq. (1) (4,14).

$$J_0 = \frac{D_J}{d_0^4}\sqrt{\frac{\sigma}{k_B T}}\exp\left[-\frac{W^*}{k_B T}\right] \quad (1)$$

The pre-exponential term in Eq. (1) includes the kinetic barrier, with D_J representing the effective diffusion coefficient controlling nucleation, whereas the exponential term corresponds to the thermodynamic barrier, which is related to the work for critical nucleus formation (W*). In Eq. (1), σ is the surface energy of the critical nucleus-liquid interface, k_B is the Boltzmann constant, $d_0 \sim \sqrt[3]{V_m/N_A}$ is the average size of the structural units, V_m is the molar volume of the crystal phase, and N_A is the Avogadro's number.

The parameter D_J can be estimated by the diffusion coefficient for viscous flow (D_η), which is given by the Eyring relation, $D_\eta = k_B T/d_0\eta$ (25,26), where η is the viscosity. Although some studies have reported the breakdown of this relation to describe crystal growth rates at low temperatures, this break has not yet been conclusively confirmed for crystal nucleation. On the other hand, for stoichiometric glasses, as the compositions used in this research, D_J is related to the transfer of structural units through the crystal nucleus/liquid interface, whereas D_η defines a cooperative mass transport process. Despite this conceptual difference, it has been shown recently that (somewhat surprisingly) the approximation given by $D_J \approx D_\eta$ seems to be valid in a lithium silicate glass in the temperature range above T_{max}, where steady-state homogeneous crystal nucleation rates are easily measurable (27). Furthermore, in liquids forming a three-dimensional network, such as the silicate glasses analyzed in this work, strong covalent and ionic bonds should be broken during viscous flow and self-diffusion processes (28). As viscosity is a property that can

be readily measured experimentally, the use of D_η is justified from a practical point of view, and for that reason, has been often used by the community, e.g. (3,7,29). Another favorable argument is that *equilibrium* viscosity is easily measured above T_g, where structural relaxation occurs very fast. Then $\eta(T)$ curves can be safely extrapolated to the low-temperature range where relaxation would play an important role. Also, the relaxation effect on viscosity can be avoided by measuring this property below T_g for a long time to assure its equilibrium value was reached.

Although a more rigorous approximation of D_J supposes the use of nucleation time-lags (τ) (30), the determination of the intrinsic values of this parameter —which only depends on the glass chemical composition and nucleation temperature —is met with many difficulties. This happens because, despite the experimental values of induction times ($t_{ind,d}$) which are measured from Nv versus time plots, being correlated with τ (Section 2.2), $t_{ind,d}$ is masked by effects of the development temperature and heating rates, which are used to grow the critical nuclei to measurable sizes. Moreover, and most significant is that they are also affected by the long relaxation times of glasses at temperatures below T_g, as demonstrated in refs. (22,23). Furthermore, τ is very short (from a few minutes to seconds) for temperatures above T_g, which makes its determination subjected to enormous errors. All these reasons led us to believe it is not possible yet to get reliable values of τ and D_τ.

An alternative procedure would be to infer the diffusivity from crystal growth rates. However, this task will be left to future research because growth rates are not available for the current glass sample batches. Therefore, to avoid these complications with τ, which would add an unwanted level of uncertainty, in this work we use experimental values of viscosity as a reasonable and widely used approximation of the diffusivity controlling nucleation. Moreover, as the alleged CNT breakdown has been reported for many oxide glass-formers using viscosity as a proxy for the effective diffusion coefficient, in this work we test the resolution of this problem by means of viscosity, which is still a reasonable assumption to exam the "experimental artifact" hypothesis for the breakdown.

Another important assumption in the CNT is related to W^*, which can be calculated considering an isotropic critical nucleus with a spherical shape, yielding $W^* = 16\pi\sigma^3/3\Delta G_v^2$, where ΔG_v is the thermodynamic driving force for crystallization per volume. In addition to assuming a sharp boundary between the crystal nuclei and the supercooled liquid, in the CNT implementation, it is also commonly assumed that the bulk properties of the critical nuclei are the same as that of

the macro-phase, and then σ is equated to the value of the interfacial energy of the planar interface (σ_∞). In other words, the interfacial energy is considered to be independent of the temperature and nucleus radius, which is known as the "capillarity" approximation (2). Hence, ΔG_v and W^* are estimated by the bulk properties of the stable phase in the CNT framework. Considering these main assumptions, Eq. (1) becomes Eq. (2), where σ is the only unknown parameter, which cannot be measured independently. Some remarks regarding σ will be discussed in Section 3.4.

$$J_0 = \frac{\sqrt{\sigma k_B T}}{d_0{}^5 \eta} \exp\left[-\frac{16\pi\sigma^3}{3k_B T \Delta G_v^2}\right] \quad (2)$$

2.2 *Nucleation Kinetics and Steady-State Criterion*

The nucleation rate (J), defined as the number of clusters that overcome the critical size per unit of time and volume (1), can be determined by taking the derivative of the crystal number density (N_v) with respect to time, $J(t) = dN_v(t)/dt$. Figure 1(a) illustrates a typical $N_v(t)$ curve, which exhibit two regions. The first of them is characterized by a transient, time-dependent nucleation rate (J(t)), whereas the second is described by a steady-state nucleation rate (J_0).

To obtain a $N_v(t)$ curve it is possible to perform single-stage (SS) or double-stage (DS) experiments. In an SS experiment, the sample is submitted to a heat treatment at a nucleation temperature (T_n) for a nucleation time (t_n), and then cooled. In a DS experiment, also known as Tammann's method (31), the sample has an additional development treatment at a temperature T_d for a period t_d, with the intention of developing the nuclei to detectable sizes via crystal growth. Ideally, the temperature T_d should be selected to minimize the dissolution of existing nuclei or the nucleation of new nuclei during the additional treatment. The size of the crystal nuclei formed at T_n is often quite small, usually below the resolution limit of microscopy techniques. Due to this, DS experiments are the most common methods used for the N_v measurement. An illustrative comparison between the $N_v(t)$ curves obtained from SS and DS heat treatments is shown in Figure 1(b).

The intercept of the asymptotic part of the $N_v(t)$ curves with the t_n-axis gives the induction time $t_{ind,n}$, for an SS, and $t_{ind,d}$, for a DS treatment, which are related to the nucleation time-lag (τ). As a result of the DS method, essentially only clusters larger than the critical size at T_d can grow in the second stage treatment (32), leading to a time shift (t_0) in the $N_v(t)$ curve, as indicated in Figure 1(b). Nevertheless, the slope of the asymptotic linear part, and consequently J_0, remains the

same. An analytical expression commonly used to describe the transient nucleation kinetics was developed by Kashchiev, Eq. (3), (33), in which the relation between τ and $t_{ind,n}$ is given by $\tau = 6.t_{ind,n}/\pi^2$.

$$N_v(t) = J_0\tau\left[\frac{t}{\tau} - \frac{\pi^2}{6} - 2\sum_{n=1}^{\infty}\frac{[-1]^n}{n^2}\exp\left(-n^2\frac{t}{\tau}\right)\right] \quad (3)$$

The main drawback of using Eq. (3) for fitting experimental $N_v(t)$ data from a DS treatment is t_0, because this expression was derived for the SS case (33). To overcome this problem, Kashchiev proposed a modified equation (Eq. (4)) (34), which is only valid for $t \geq t_0$, where t is replaced by $(t - t_0)$, and the times τ and $t_{ind,d}$ become correlated by $\tau = 6(t_{ind,n} - t_0)/\pi^2$.

$$N_v(t) = J_0\tau\left[\frac{t-t_0}{\tau} - \frac{\pi^2}{6} - 2\sum_{n=1}^{\infty}\frac{[-1]^n}{n^2}\exp\left(-n^2\frac{t-t_0}{\tau}\right)\right] \quad (4)$$

As shown in Figure 2(a) and (b), a short t_n could lead to an underestimation in J_0 if the nucleation rate is estimated at the early stages of its evolution in a transient condition. At temperatures T_n below T_{max}, where the CNT allegedly fails, this underestimation could be even more significant because the crystal nucleation kinetics is relatively slow.

For this reason, a steady-state criterion is needed to increase the confidence of the analysis. According to Shneidman (35), experimental points for which the ratio J/J_0 is higher than 0.93 are sufficiently close to steady-state conditions. In Kashchiev`s framework, this condition is reached when $(t - t_0)/\tau > 3.3$, as shown schematically in Figure (2c). This criterion was implemented for the first time in (15) and is also considered in our analysis in this paper (Section 4.2 and supplementary material).

3 Materials and Methods

3.1 *Glass Preparation*

Three glass batches were used in this work, lithium disilicate ($Li_2Si_2O_5$), barium disilicate ($BaSi_2O_5$), and soda-lime-silica ($Na_4CaSi_3O_9$). They all undergo homogeneous crystal nucleation

in laboratory time scales (11,36,37), and their liquid has the same chemical composition as the most stable crystalline phase, which makes them interesting substances for studying nucleation kinetics. The chemicals used to synthesize these glasses are summarized in Table S1 (Supplementary Material). The glasses $Li_2Si_2O_5$ and $BaSi_2O_5$ were prepared in the previous studies of Deubener et al. (32), and Zanotto (3,36), respectively, and the methodology used to obtain them can be found therein. In references (3,36) the $BaSi_2O_5$ glass used in this work is identified as 33.2C. Detailed information regarding the chemical analysis procedures for the $Li_2Si_2O_5$ and $BaSi_2O_5$ glasses can be found in references (32) and (36), respectively.

The nominal chemical mixture for the $Na_4CaSi_3O_9$ glass was prepared following the conventional melting/splat cooling method. Before melting, the reagents were mixed and calcined at 1123 K for 10 h to decompose sodium and calcium carbonates. Thereafter, the reactant mixture was melted in Pt crucibles at 1573 K and then quenched, crushed and re-melted to promote chemical homogeneity. This procedure was repeated twice. Finally, the melt was quenched between two steel plates to obtain small pieces of approximately 2–3 mm thick glasses. To avoid incipient nucleation, no annealing treatment was performed. To determine the chemical composition, $Na_4CaSi_3O_9$ glass was analyzed by X-ray fluorescence. Differential scanning calorimetry was used (Netzsch DSC 404) to determine the glass transition temperature (T_g) of the glasses. The analyses were performed in monolithic bulk samples of ~ 25 mg, using a Pt crucible with lid, at a heating rate of 10 K/min, under air atmosphere.

3.2 *Nucleation Rate Measurements*

The experimental $N_v(t)$ curves were determined at different T_n, using the DS method (Section 2.2). Samples of approximately 4 × 4 × 3 mm^3 were initially heat-treated at T_n into a vertical furnace with a precision of ±1 K. The T_n range was 715 to 753 K for $Li_2Si_2O_5$, 943 to 1038 K for $BaSi_2O_5$, and 738 to 793 K for $Na_4CaSi_3O_9$. Thus, we have covered temperature ranges of approximately 20-25 K below and 30-50 K above the reported T_{max}. The T_d were 865 (t_d = 4 to 15 min), 1088 (t_d = 4 to 9 min), and 843 K (t_d = 2.5 to 9 min), respectively. These T_d are above the temperature range reported in the literature where we would expect a significant nucleation rate (4,11,36,37). Although it is presumed that the thermal history of the samples has an effect on the measured N_v values, we argue that such effect (if present) will not alter the value of J_0 if t_n is long enough to reach the steady-state nucleation (32). Moreover, in our analysis all the heat treatments were performed in the same furnace with the same T_d for each glass, and the sample sizes were practically equal. Additionally, the estimated time to reach the thermal equilibrium at the

development temperatures used for the glasses analyzed in this study is around 50 s.

After the DS heat treatment, the samples were ground with SiC paper (320, 400, 500, 600, and 1200 grit) to remove the surface crystalline layer and then polished with a micrometric CeO_2 powder aqueous suspension. To reveal the crystals on the specimen surfaces, the $Li_2Si_2O_5$ samples were submitted to an ultrasonic bath (37 kHz) in water for ~10 min, whereas the $BaSi_2O_5$ samples were etched in a 2% HF (vol%) solution for ~1.5 min. Samples of the $Na_4CaSi_3O_9$ glass did not require any additional procedure to reveal the crystals.

The samples' cross-sections were analyzed by reflected light optical microscopy (LEICA DMRX coupled with a LEICA DFC490 camera) to estimate the number of crystals per unit area (N_s). The measured crystal number density (N_v^m) is related to the average of N_s ($\overline{N}_s$) through Eq. (5) (38).

$$N_v^m = \frac{2}{\pi K(q)} \overline{N}_s \bar{z} \tag{5}$$

Here $\bar{z}$ is the average of the reciprocal of the minor axis of the largest crystal traces detected and K(q), given by Eq. (6) (38), is a function of the aspect ratio of the largest crystals (q).

$$K(q) = \frac{1}{q} + \frac{q \ln\left[\left(1 + \sqrt{1 - q^2}\right)/q\right]}{\sqrt{1 - q^2}} \tag{6}$$

In this work, $\overline{N}_s$ was determined by counting at least 300 crystals for each t_n and T_n considered. As shown in Figure 3, the $Li_2Si_2O_5$ crystals have a prolate ellipsoidal shape, the $BaSi_2O_5$ crystals are irregular, but their geometry can be considered circular, and the $Na_4CaSi_3O_9$ crystals have a spherical form. Then, K(q) ~ 1 if assuming spherical crystals for the $BaSi_2O_5$ and $Na_4CaSi_3O_9$ glasses, whereas K(q) ≠ 1 for $Li_2Si_2O_5$. As the use of reflected light optical microscopy could lead to an underestimation of N_s, due to crystal traces in the micrographs that are smaller than the microscope resolution limit ε (~ 0.3 to ~ 0.5 μm, depending on the numerical aperture of the microscope objective), we used Eq. (7) to calculate the underestimated fraction (f) (39), and Eq. (8) to determine the real value of N_v. In Eq. (7), D_M is the largest dimension of the larger crystal traces in the polished cross-sections.

$$f = \frac{2}{\pi}\sin^{-1}\left(\frac{\varepsilon}{D_M}\right) \quad (7)$$

$$N_v = \frac{N_v^m}{1-f} \quad (8)$$

3.3 *Viscosity Measurements*

In our analysis, we consider that the diffusion coefficient that governs the crystal nucleation process (D_J) is equal to the effective diffusion coefficient that controls the viscous flow (D_η) through the Eyring relation, shown in Section 2.1. Thus, we measured the shear viscosity (η) of supercooled $Li_2Si_2O_5$ and $Na_4CaSi_3O_9$ liquids in the range of 10^8 to 10^{14} Pa.s, using a homemade penetration viscometer with a rigid Nimonic 80A indenter. The reliability of the viscosity values higher than 10^{12} Pa.s is based on the experimental time used for the measurements, which were 3 h for the $Li_2Si_2O_5$ ($\eta \sim 10^{13}$ Pa.s) and 20 h for the $Na_4CaSi_3O_9$ glasses ($\eta \sim 10^{14}$ Pa.s). According to the values reported in (40), these times are long enough to achieve the equilibrium viscosity in silicate glasses. Similar measurements of η were performed previously in ref. (36) for the $BaSi_2O_5$ glass used in this work and further information about the experimental procedure can be found therein. To avoid the influence of minor chemical compositional changes and glass preparation conditions, all the viscosity measurements were carried out in samples obtained from the same batch used for the nucleation experiments. With these considerations, the corresponding experimental $\eta(T)$ data were fitted with the MYEGA (Mauro-Yue-Ellison-Gupta-Allan) model, Eq. (9) (41).

$$\log_{10}(\eta) = \log_{10}(\eta_\infty) + \frac{T_{12}}{T}[12 - \log_{10}(\eta_\infty)]\exp\left(\left[\frac{m}{12 - \log_{10}(\eta_\infty)} - 1\right]\left[\frac{T_{12}}{T} - 1\right]\right) \quad (9)$$

The MYEGA equation is presented here in terms of physically meaningful parameters η_∞, T_{12}, and m, which represent the extrapolated viscosity in the limit of infinite temperature, the temperature where the shear viscosity is 10^{12} Pa.s ($T_{12} \sim T_g$ in laboratory experiments), and the liquid fragility index, respectively.

It is worth noting that using experimental (nucleation and viscosity) data from the *same* glass batch was a relevant experimental design choice because dynamic properties are affected by the

procedural and environmental conditions of glass preparation, such as the water (OH^-) content (42,43), slight departures from the intended stoichiometric composition (44), and the presence of impurities, which vary from batch to batch (45). For instance, it is well-known that the increase in the OH^- content not just reduces the viscosity (42), but also reduces the thermodynamic barrier for nucleation (43) and significantly increases the nucleation rates. Therefore, using samples of the *same* glass batch for crystallization and viscosity measurements allows a much more reliable analysis, by avoiding complications caused by structural and compositional variables.

3.4 *CNT "Breakdown" Test*

To test the CNT according to the assumptions made in Section 2.1 (see Eq. (2)), it is necessary to know the values of $\eta(T)$ and J_0 for each T_n. The first can be computed using a regression of Eq. (9) on experimental data, and the latter is obtained from fitting the $N_v(t)$ experimental curves with Eq. (4). To verify the steady-state condition of the different isothermal nucleation treatments, we used the steady-state criterion explained in Section 2.2. Thus, only the $N_v(t)$ datasets that fulfil the established criterion were used in the CNT analysis. With $\eta(T)$ and J_0, we tested the CNT using two different methods described in the following two paragraphs. The first method consists of the linearization of Eq. (2), given by Eq. (10), where $A = \sqrt{\sigma k_B}/d_0^5$ and $B = 16\pi\sigma^3/3k_B$. In this case, it is assumed that σ is temperature-independent, as established by the capillarity approximation (2). A linear temperature dependence in the whole range indicates absence of a "CNT breakdown", otherwise the existence of a nucleation breakdown is considered. The thermodynamic driving force ΔG_v was calculated according to the approximated expression $\Delta G_v V_m = \Delta H_m((T-T_m)/T_m)$ where ΔH_m is the heat of fusion and T_m is the melting temperature (4). This approximation considers the specific heats of the supercooled liquid and crystal to be similar and give an upper bound for ΔG_v.

$$\ln\left(\frac{\eta J_0}{\sqrt{T}}\right) = \ln(A) - \frac{B}{T\Delta G_v^2} \qquad (10)$$

The second method avoids the capillarity approximation, considering the temperature dependence of σ given by Eq. (11). This relation comes from Eq. (2) and it was solved according to the numerical solution proposed in ref. (46). In this case, a monotonically increase of $\sigma(T)$ allows us to infer that the CNT is self-consistent with the assumptions made in this research.

$$\sigma(T) = \sqrt[3]{-\frac{kT\Delta G_V^2}{32\pi} W_{-1}\left(-\frac{32\pi d_0^{30}}{\Delta G_V^2}\left[\frac{1}{kT}\right]^4 [J_0\eta]^6\right)} \quad (11)$$

In the previous equation, W_{-1} is the Lambert W function computed in the −1 branch. The non-linear fits of Eqs. (4) and (9) to the experimental data of $N_v(t)$ and $\eta(T)$, respectively, as well as the estimative of $\sigma(T)$ indicated by Eq. (11) were carried out using the Python programming language. The procedures for the fittings are available in the open-source module GlassPy (47). It is worth mentioning that two different uncertainty calculations were performed in this work. The error propagation was computed using the Python uncertainties module (48), and the confidence bands were obtained using a Taylor expansion of the error in the y-axis following the method reported by Wolberg (49). This computation was done using the lmfit Python module (50), which, in turn, is based on a code from the Kapteyn Package (51).

4 Results and Discussion

4.1 *Glass Characterization*

The values of T_g measured for the $Li_2Si_2O_5$, $BaSi_2O_5$, and $Na_4CaSi_3O_9$ glasses were 728, 968, and 747 K, respectively, as shown in the DSC curves (Figure 4). The chemical compositions of the 3 glasses are close to the nominal stoichiometries (see Supplementary Material, Tables S2-S4).

4.2 *Steady-State Criterion*

We analyzed the $N_v(t)$ experimental datasets (see Supplementary file) by non-linear regressions of Eq. (4) to obtain the steady-state nucleation rates (see Supplementary Material, Figures S1-S3). It must be noted that the nonlinear regression of the $N_v(t)$ experimental data for the $BaSi_2O_5$ glass at 943 K (the lowest temperature for this composition, shown in Figure S2a) is peculiar. The six data points measured at the highest times are systematically higher than the nonlinear regression. Statistically, this is due to the combination of many data points for lower times with low uncertainty, and few data points of longer times with high uncertainty. However, this strange result could be an indication that the steady-state was not reached for this dataset, even though it passed the steady-state test discussed in Section 2.2. Fortunately, most of the error bars of the said six points lie within the confidence bands (even if some of the actual points are close to but outside the bands).

In order to have a better observation of the initial stages of nucleation, the $N_v(t)$ curves are

also available in log scale in the Supplementary Material (Figures S4-S6). With this procedure, we were able to obtain the temperature dependence of J_0, shown in Figure 5(a-c), where the dotted blue lines indicate the temperature of the maximum homogeneous nucleation rate (T_{max}).

As already discussed, one critical requirement to test the alleged breakdown of CNT is that the system has data that have reached the steady-state regime, otherwise J_0 would be underestimated. For this reason, we evaluated the evolution of the reduced nucleation rate (J/J_0) as shown in Figure 6(a-c), to verify if the experimental nucleation time used for the $N_v(t)$ measurements were close to the time required to reach the steady-state.

The master curve $N_v/J_0\tau$ versus $(t - t_0)/\tau$ for each glass (Eq. (4)) is also shown in Figure 6(a-c). It can be observed that all the $N_V(t)$ measurements for the three glasses passed the steady-state criterion (i.e., at least one data point for which $J/J_0 \geq 93\%$, Section 3.4), for all the considered nucleation temperatures, indicated by the dotted blue lines. The importance in establishing a steady-state criterion can be appreciated by comparing the results reported in ref. (11), which strongly suggest the existence of the CNT breakdown for $BaSi_2O_5$ and $Ba_5Si_8O_{21}$ glasses, with those presented in (16) for the same group, demonstrating that the break "disappears" in the $Ba_5Si_8O_{21}$ glass, once t_n is considerably extended. Similarly, as indicated in (15), the steady-state regime was *not* achieved at the lowest nucleation temperatures in some experimental $N_V(t)$ data from studies that reported the alleged nucleation break for $Li_2Si_2O_5$ and $Na_4CaSi_3O_9$ glasses. Thus, these studies suggest that a steady-state criterion is highly recommendable to avoid wrong conclusions upon nucleation theories.

4.3 *Diffusion Mechanism*

To determine $\eta(T)$, regressions of Eq. (9) to experimental viscosity data were performed, as shown in 7(a-c), and the regression parameters are summarized in Table 1.

Owing to the lack of viscosity data near T_m, the uncertainty in $\log_{10}(\eta_\infty)$ is large. However, this factor does not affect our analysis because the extrapolations of viscosity are small (Figure 7 shows the whole range of the viscosity data used in this study, including eventual extrapolations).

4.4 *CNT "Breakdown" Test*

Taking into account all the theoretical and experimental considerations previously discussed, we tested the existence of the CNT breakdown, to check whether its alleged failure below T_{max}—claimed by several authors (6,8–11) —persists. The CNT test was initially developed considering the crystal/liquid interfacial energy (σ) as being temperature-independent, according to the

capillarity approximation of CNT (52). The result of this test, Figure 8(a-c), indeed shows a linear behavior of the experimental data, where, within the confidence bands, all of the data points are well described by the linearization of the CNT (Eq. (10)) with *no break*. Additionally, for the sake of comparison, we made an analysis of the CNT using only the results for T_n in which it was possible to get a reasonable value of τ (where the standard deviation of τ is lower than τ itself). As can be seen from Figure S7 in the supplementary material, using this strategy, only the $BaSi_2O_5$ glass presents some weak evidence of the alleged "breakdown" of CNT. Even so, this analysis is not as conclusive as that conducted by assuming $D \approx D\eta$, since we could not use all the experimental nucleation data to evaluate the CNT validity.

On the other hand, as σ is a thermodynamic property, it is expected to have a certain temperature dependence. Moreover, due to the nano-size of the critical nuclei, a significant part of the structural units of the critical nuclei lies in the crystal/liquid interfacial region. Hence, the nucleation process can be understood as a surface phenomenon (53). Accordingly, the temperature dependence of σ given by Eq. (11) is an alternative way to test the CNT break. As can be observed in Figure 9(a-c), by force-fitting σ individually to all data points, this property shows a slight positive increase with temperature, which is expected if the CNT is consistent with the considered framework (13,54,55), supporting that there is *no break* of the CNT at T_{max}. Figures 8(c) and 9(c) show that the uncertainty for the experimental data of the $Na_4CaSi_3O_9$ composition at the highest temperature is larger than those at lower temperatures. This is a consequence of the broad confidence band resulting from the nonlinear fit of the viscosity experimental data in Figure 7(c) via Eq. (9), since at this temperature range this glass crystallizes easily, hindering the measurement of the equilibrium viscosity.

The monotonic dependence of σ has also been reported for other single (54,56) and multi-component systems (57), in molecular dynamics simulations and laboratory experiments, respectively. In these studies, this behavior has been associated with the curvature dependence of the critical nuclei with the temperature. A diffuse interface, suggested by the DIT, between the critical nucleus and the liquid has also been claimed to be the cause of the positive temperature dependence of σ (58). Besides that, some studies mention that the behavior of $\sigma(T)$ could be linked with an entropy decrease in the parental liquid phase, whose order gradually increases in the proximity of the newly formed phase (4,55). Finally, it should be pointed out that, since there is no experimental method for measuring σ directly, a comparison of calculated and actual σ is not feasible (54).

Summarizing, none of the tests shown in Figure 8(a-c) and 9(a-c) show any evidence of the alleged discrepancy between the experimental data and the CNT predictions below T_{max}. This result, considering new experimental data for 3 systems, supports the hypothesis that the nucleation break is just an *experimental artifact*, not an intrinsic phenomenon. The reported break in previous studies was most likely a consequence of the mixture of viscosity and nucleation data from different glass batches and, most importantly, underestimation in J_0 (i.e., data below T_g that have not reached the steady-state regime). Our findings are in line with the results of (15), where the same hypothesis was tested using literature data and indicated that the CNT breakdown at T_{max} is simply an artifact. They also agree with the results of Xia et al. (16).

Furthermore, although a CNT test at even deeper undercooling below T_{max} would be quite interesting, such trials have experimental limitations, such as the very long nucleation times needed to reach the steady-state regime at very low temperatures, which could take several months (27), and crystal impingement, precluding a reliable experimental measure of N_v. Nevertheless, our results are well grounded by recent experimental (15,16,29) and molecular dynamics simulation (54,59,60) studies, that demonstrate the validity of CNT for the description and prediction of crystal nucleation rates in supercooled liquids.

5 Summary and Conclusions

To confirm whether the so-called nucleation break at $T_{max} \sim T_g$ was an experimental artifact due to the use of datasets that have not reached the steady-state regime below T_{max}, we tested the Classical Nucleation Theory using a plethora of new experimental data for three stoichiometric glasses: $Li_2Si_2O_5$, $BaSi_2O_5$ and $Na_4CaSi_3O_9$. All nucleation rate and viscosity measurements were performed using samples of the same glass batch for each system, a steady-state criterion was applied, and the error propagation was calculated.

There was *no* sign of the break in a temperature range covering 20-25 K below and 30-50 K above the reported experimental T_{max} with this rigorous procedure. Thus, our results validate the hypothesis that the alleged CNT failure below T_g is just a consequence of using too short experimental nucleation times, which are insufficient to reach the steady-state regime. The present results corroborate recent experimental and MD simulation studies that demonstrated the validity of CNT to describe nucleation rates in supercooled liquids.

Acknowledgments

This study was financed in part by the Coordenação de Aperfeiçoamento de Pessoal de Nível Superior - Brasil (CAPES) - Finance Code 001. The authors are grateful to the Brazilian agencies: National Council for Scientific and Technological Development (CNPq), grant numbers 141057/2017-3 (MHRA) and 141816/2018-0 (LRR), and to the São Paulo State Research Foundation (FAPESP), grants 2013/07793-6 (CEPID) and 2017/12491-0 (DRC) for the financial support received. Finally, we would like to thank Vladimir M. Fokin for his valuable help with some measurements and discussions.

Authorship contribution statement

Maria Helena Ramírez Acosta (Main Author):

Conceptualization
Investigation
Methodology
Formal Analysis
Writing - original draft
Writing - review & editing

Lorena Raphael Rodrigues (Contributor):

Conceptualization
Investigation
Methodology
Formal Analysis
Writing - review & editing

Daniel Roberto Cassar (Contributor):

Conceptualization
Data curation
Formal analysis
Methodology

Software

Visualization

Writing – review & editing

Maziar Montazerian (Contributor):

Investigation

Writing – review & editing

Oscar Peitl Filho (Contributor):

Investigation

Edgar Dutra Zanotto (Advisor):

Conceptualization

Funding acquisition

Project administration

Resources

Supervision

Formal Analysis

Writing – review & editing

References

1. Kelton K, Greer AL. Nucleation in condensed matter: applications in materials and biology. Vol. 15. Oxford: Elsevier; 2010.
2. Karthika S, Radhakrishnan TK, Kalaichelvi P. A Review of Classical and Nonclassical Nucleation Theories. Cryst Growth Des. 2016;16:6663–81.
3. Zanotto ED, James PF. Experimental tests of the classical nucleation theory for glasses. J Non Cryst Solids. 1985;74(2–3):373–94.
4. Fokin VM, Zanotto ED, Yuritsyn NS, Schmelzer JWP. Homogeneous crystal nucleation in silicate glasses: A 40 years perspective. J Non Cryst Solids. 2006;352(26–27):2681–714.
5. Manrich S, Zanotto ED. Nucleação de cristais em silicatos vítreos analisada através de

diferentes formas da teoria clássica. Cerâmica. 1995;41:105–9.
6. James PF. Kinetics of crystal nucleation in silicate glasses. J Non Cryst Solids. 1985;73(1–3):517–40.
7. Fokin VM, Zanotto ED, Schmelzer JWP. Homogeneous nucleation versus glass transition temperature of silicate glasses. J Non Cryst Solids. 2003;321:52–65.
8. Weinberg MC, Zanotto ED. Re-examination of the temperature dependence of the classical nucleation rate: homogeneous crystal nucleation in glass. J Non Cryst Solids. 1989;108(1):99–108.
9. Fokin VM, Abyzov AS, Zanotto ED, Cassar DR, Rodrigues AM, Schmelzer JWP. Crystal nucleation in glass-forming liquids: Variation of the size of the "structural units" with temperature. J Non Cryst Solids. 2016;447:35–44.
10. Abyzov AS, Fokin VM, Yuritsyn NS, Rodrigues AM, Schmelzer JWP. The effect of heterogeneous structure of glass-forming liquids on crystal nucleation. J Non Cryst Solids. 2017;462:32–40.
11. Xia X, Van Hoesen DC, McKenzie ME, Youngman RE, Gulbiten O, Kelton KF. Time-dependent nucleation rate measurements in BaO· 2SiO2 and 5BaO· 8SiO2 glasses. J Non Cryst Solids. 2019;525:119575.
12. Soares Jr PC, Zanotto ED, Fokin VM, Jain H. TEM and XRD study of early crystallization of lithium disilicate glasses. J Non Cryst Solids. 2003;331(1–3):217–27.
13. Abyzov AS, Fokin VM, Mendes A, Zanotto ED, Schmelzer JWP. The effect of elastic stresses on the thermodynamic barrier for crystal nucleation. J Non Cryst Solids. 2016;432:325–33.
14. Gupta PK, Cassar DR, Zanotto ED. Role of dynamic heterogeneities in crystal nucleation kinetics in an oxide supercooled liquid. J Chem Phys. 2016;145:211920.
15. Cassar DR, Serra AH, Peitl O, Zanotto ED. Critical assessment of the alleged failure of the Classical Nucleation Theory at low temperatures. J Non Cryst Solids. 2020;547:120297.
16. Xia X, Hoesen DC Van, Mckenzie ME, Youngman RE, Kelton KF. Low-temperature nucleation anomaly in silicate glasses shown to be artifact in a 5BaO·8SiO2 glass. Nat Commun. 2021;12:2026:1–6.
17. Cassar DR, Zanotto ED. Transport mechanism in crystal nucleation in oxide glass-formers. In: Glass & Optical Materials Division, Annual Meeting. San Antonio, TX; 2018.
18. Cassar DR, Serra AH, Rodrigues AM, Zanotto ED. Reanalyzing crystal nucleation data: A

step back to move forward. In: 25th International Congress on Glass (ICG). Boston: 25th International Congress on Glass (ICG); 2019.

19. Ramírez MH, Zanotto ED. Unmasking the Breakdown of the Classical Nucleation Theory. In: 25th International Congress on Glass (ICG). Boston: 25th International Congress on Glass (ICG); 2019.
20. Cassar DR, Serra AH, Peitl O, Rodrigues AM, Zanotto ED. The failure of the Classical Nucleation Theory at low temperatures resolved. arXiv Prepr arXiv:190203193v1. 2019;1–34.
21. Xia X, Hoesen DC Van, Mckenzie ME, Youngman RE, Kelton KF. The Low-Temperature Nucleation Rate Anomaly in Silicate Glasses is an Artifact. arXiv Prepr arXiv:200504845. 2020;
22. Schmelzer JWP, Tropin T V., Fokin VM, Abyzov AS, Zanotto ED. Effects of glass transition and structural relaxation on crystal nucleation: Theoretical description and model analysis. Entropy. 2020;22(10):1–36.
23. Fokin VM, Abyzov AS, Yuritsyn NS, Schmelzer JWP, Zanotto ED. Effect of structural relaxation on crystal nucleation in glasses. Acta Mater. 2021;203:9–11.
24. Gibbs JW. On the equilibrium of heterogeneous substances. Trans Connect Acad ARTS Sci. 1878;s3-16(96):441–58.
25. Einstein A. On the Motion of Small Particles Suspended in Liquids at Rest Required by the Molecular-Kinetic Theory of Heat. Ann Phys. 1905;17:549–60.
26. Eyring H. Viscosity, Plasticity, and Diffusion as Examples of Absolute Reaction Rates. J Chem Phys. 1936;4:283–91.
27. Fokin VM, Abyzov AS, Rodrigues AM, Pompermayer RZ, Macena GS, Zanotto ED, et al. Effect of non-stoichiometry on the crystal nucleation and growth in oxide glasses. Acta Mater. 2019;180:317–28.
28. Turnbull D, Cohen MH. Concerning reconstructive transformation and formation of glass. J Chem Phys. 1958;29(5):1049–54.
29. Huang C, Chen Z, Gui Y, Shi C, Zhang GGZ, Yu L. Crystal nucleation rates in glass-forming molecular liquids: D-sorbitol, D-arabitol, D-xylitol, and glycerol. J Chem Phys. 2018;149(5).
30. Fokin VM, Schmelzer JWP, Nascimento MLF, Zanotto ED. Diffusion coefficients for crystal nucleation and growth in deeply undercooled glass-forming liquids. J Chem Phys.

2007;126(23):234507.

31. Tammann G. Über die Abhängigkeit der Zahl der Kerne, welche sich in verschiedenen unterkühlten Flüssigkeiten bilden, von der Temperatur. Zeitschrift für Phys Chemie. 1898;25(1):441–79.
32. Deubener J, Montazerian M, Krüger S, Peitl O, Zanotto ED. Heating rate effects in time-dependent homogeneous nucleation in glasses. J Non Cryst Solids. 2017;474:1–8.
33. Kashchiev D. Nucleation at existing cluster size distributions. Surf Sci. 1969;18:389–97.
34. Kashchiev D. Nucleation: basic theory with applications. Oxford: Elsevier; 2000.
35. Shneidman VA. Establishment of a steady-state nucleation regime. Theory and comparison with experimental data for glasses. SovPhysTechPhys. 1988;33(11):1338–42.
36. Zanotto ED. The effects of amorphous phase separation on crystal nucleation in baria-silica and lithia-silica glasses. University of Sheffield; 1982.
37. Kalinina AM, Filipovich VN, Fokin VM. Stationary and non-stationary crystal nucleation rate in a glass of 2Na2O.CaO.3SiO2 stoichiometric composition. J Non Cryst Solids. 1980;38/39:723–8.
38. DeHoff RT, Rhines FN. Determination of number of particles per unit volume from measurements made on random plane sections: the general cylinder and the ellipsoid. Trans Met Soc AIME. 1961;221(5):975–82.
39. Zanotto ED, James PF. A theoretical and experimental assessment of systematic errors in nucleation experiments. J Non Cryst Solids. 1990;124(1):86–90.
40. Sipp A, Neuville DR, Richet P. Viscosity, configurational entropy and relaxation kinetics of borosilicate melts. J Non Cryst Solids. 1997;211(3):281–93.
41. Mauro JC, Yue Y, Ellison AJ, Gupta PK, Allan DC. Viscosity of glass-forming liquids. Proc Natl Acad Sci [Internet]. 2009;106(47):19780–4. Available from: http://www.pnas.org/cgi/doi/10.1073/pnas.0911705106
42. James PF, Gonzalez-Oliver CJR, Johnson PS, James PF. Influence of water content on the rates of crystal nucleation and growth in lithia-silica and soda-lime-silica glasses. J Mater Sci. 1979;14(5):1159–69.
43. Davis MJ, Ihinger PD, Lasaga AC. Influence of water on nucleation kinetics in silicate melt. J Non Cryst Solids. 1997;219:62–9.
44. Deubener J. Compositional onset of homogeneous nucleation in (Li, Na) disilicate glasses. J Non Cryst Solids. 2000;274(1):195–201.

45. Thieme K, Avramov I, Rüssel C. The mechanism of deceleration of nucleation and crystal growth by the small addition of transition metals to lithium disilicate glasses. Sci Rep. 2016;6:25451.
46. Cassar DR. Solving the classical nucleation theory with respect to the surface energy. 2019;511(January):183–5.
47. Cassar DR. drcassar/glasspy: GlassPy 0.3, Zenodo [Internet]. 2020. Available from: https://zenodo.org/record/3930351
48. Lebigot EO. Uncertainties: a Python package for calculations with uncertainties [Internet]. [cited 2014 Mar 27]. Available from: http://pythonhosted.org/uncertainties/
49. Wolberg J. Data analysis using the method of least squares: extracting the most information from experiments. 2006;
50. Newville M, Stensitzki T, Allen DB, Ingargiola A. LMFIT: Non-Linear Least-Square Minimization and Curve-Fitting for Python (Version 0.8.0). Zenodo; 2014.
51. Terlouw JP, Vogelaar MGR. Kapteyn package, version 3 (Groningen). 2019.
52. Kalikmanov VI. Classical nucleation theory. In: Nucleation theory. Springer; 2013. p. 17–41.
53. Baidakov VG, Tipeev AO. Crystal nucleation and the solid–liquid interfacial free energy. J Chem Phys. 2012;136:074510.
54. Tipeev AO, Zanotto ED, Rino JP. Diffusivity, Interfacial Free Energy, and Crystal Nucleation in a Supercooled Lennard-Jones Liquid. J Phys Chem C. 2018;122(50):28884−28894.
55. Schmelzer JWP, Abyzov AS, Baidakov VG. Entropy and the Tolman Parameter in Nucleation Theory. Entropy. 2019;21(7):1–45.
56. Sun Y, Zhang F, Song H, Mendelev MI, Wang C-Z, Ho K-M. Temperature dependence of the solid-liquid interface free energy of Ni and Al from molecular dynamics simulation of nucleation. J Chem Phys. 2018;149(17):174501.
57. Fokin VM, Zanotto ED. Crystal nucleation in silicate glasses: the temperature and size dependence of crystal/liquid surface energy. J Non Cryst Solids. 2000;265:105–12.
58. Gránásy L. Diffuse interface model of crystal nucleation. J Non Cryst Solids. 1997;219:49–56.
59. Prado SCC, Rino JP, Zanotto ED. Successful test of the classical nucleation theory by molecular dynamic simulations of BaS. Comput Mater Sci. 2019;161:99–106.

60. Separdar L, Rino JP, Zanotto ED. Molecular dynamics simulations of spontaneous and seeded nucleation and theoretical calculations for zinc selenide. Comput Mater Sci. 2021;187:110124.

Figure Captions

Figure 1. (a) Crystal number density versus time showing the time-dependent and steady-state nucleation rate and (b) schematic comparison of $N_v(t)$ curves obtained from single- and double-stage heat treatments.

Figure 2. Crystal number density versus nucleation time showing a (a) transient and a (b) steady-state condition for the same T_n, where $t_{ind,1} < t_{ind,2}$ and $J_1 < J_2$ and (c) time dependence of the reduced nucleation rate, $J(t)/J_0$, for the modified Kashchiev expression, Eq. (4).

Figure 3. Reflected light optical micrographs of (a) $Li_2Si_2O_5$ glass treated at T_n = 745 K for 19 h and T_d = 865 K for 15 min, (b) $BaSi_2O_5$ treated at T_n = 943 K for 6 h and T_d = 1088 K for 8 min and (c) $Na_4CaSi_3O_9$ treated at T_n = 738 K for 13 h and T_d = 843 K for 2.5 min.

Figure 4. DSC curves for (a) $Li_2Si_2O_5$, (b) $BaSi_2O_5$, and (c) $Na_4CaSi_3O_9$ glasses obtained at a heating rate of 10 K/min.

Figure 5. Steady-state nucleation rates as a function of the temperature obtained by fitting Eq. (4) to the $N_v(t)$ experimental datasets for (a) $Li_2Si_2O_5$, (b) $BaSi_2O_5$ and (c) $Na_4CaSi_3O_9$ glasses. The data uncertainty is two standard deviations. The dotted blue vertical lines indicate T_{max}.

Figure 6. Reduced nucleation rate, J/J_0 (black curve, right hand side axis), and reduced crystal density, curve $N_v/J_0\tau$ (dashed red curve, left hand side axis), as a function of the reduced time, $(t - t_0)/\tau$, for (a) $Li_2Si_2O_5$, (b) $BaSi_2O_5$, and (c) $Na_4CaSi_3O_9$ glasses. The data uncertainty is one standard deviation. The dotted blue lines indicate the maximum

experimental nucleation time in decreasing order of nucleation temperature, from right to left. The horizontal gray line refers to the relation $J/J_0 \geq 93\%$.

Figure 7. Shear viscosity as a function of temperature for (a) $Li_2Si_2O_5$, (b) $BaSi_2O_5$ and (c) $Na_4CaSi_3O_9$ glasses. The continuous red line corresponds to the fit of Eq. (9) to the $\eta(T)$ experimental data represented by black dots. The dashed grey lines show the regression confidence bands (95%), whereas the dotted vertical blue lines indicate the T_{max}.

Figure 8. Analysis of the classical nucleation equation for (a) $Li_2Si_2O_5$, (b) $BaSi_2O_5$ and (c) $Na_4CaSi_3O_9$ glasses assuming $D_J \approx D_\eta$ and σ as a temperature-independent parameter. The continuous red line corresponds to the linear regression. The uncertainty of the data is two standard deviations, and the 95% confidence bands are given by the dashed gray line. The dotted vertical blue lines show the T_{max} and the orange dash-dotted vertical lines indicate T_g.

Figure 9. Temperature dependence of interfacial energy calculated from nucleation data for (a) $Li_2Si_2O_5$, (b) $BaSi_2O_5$ and (c) $Na_4CaSi_3O_9$ glasses. The vertical dotted blue lines indicate the temperatures of maximum nucleation rates, T_{max}.

Tables

Tabla 1. Parameters T_{12}, *m* and $\log_{10}(\eta_\infty)$ obtained from fits of Eq. (9) to $\eta(T)$ experimental data. The uncertainty is one standard deviation.

Composition	T_{12} [K]	*m*	$\log_{10}(\eta_\infty)$
$Li_2Si_2O_5$	734.5(4)	43(1)	-7(9)
$BaSi_2O_5$	959(1)	52(3)	3(2)
$Na_4CaSi_3O_9$	745(1)	52(2)	-14(35)

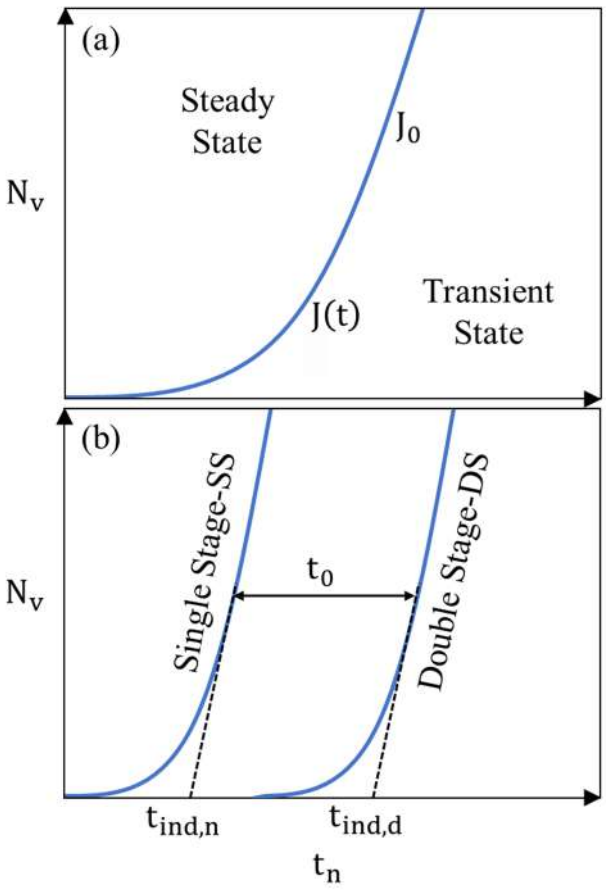

jace_17852_f1.tif

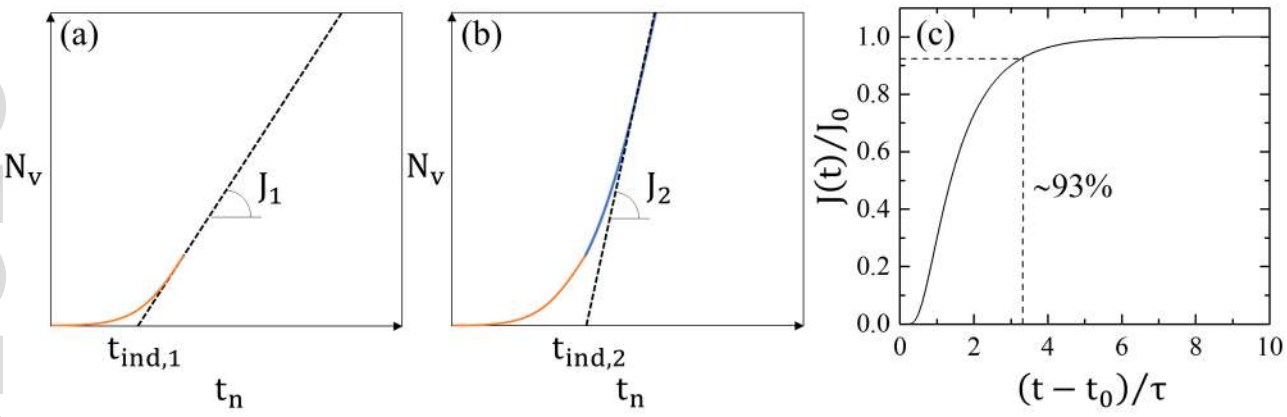

jace_17852_f2.tif

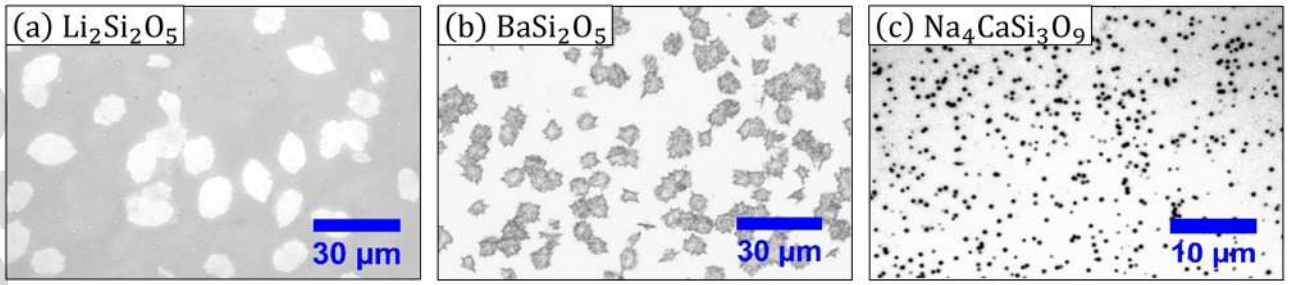

jace_17852_f3.tif

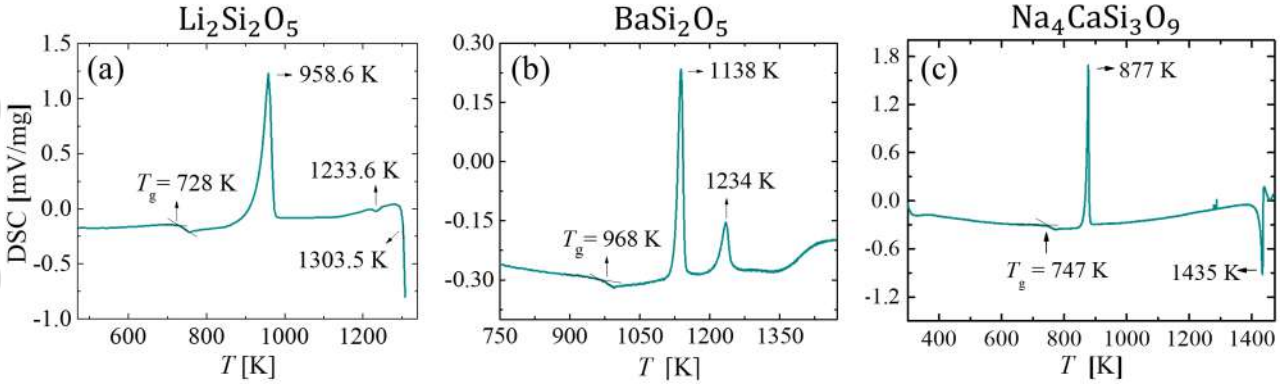

jace_17852_f4.tif

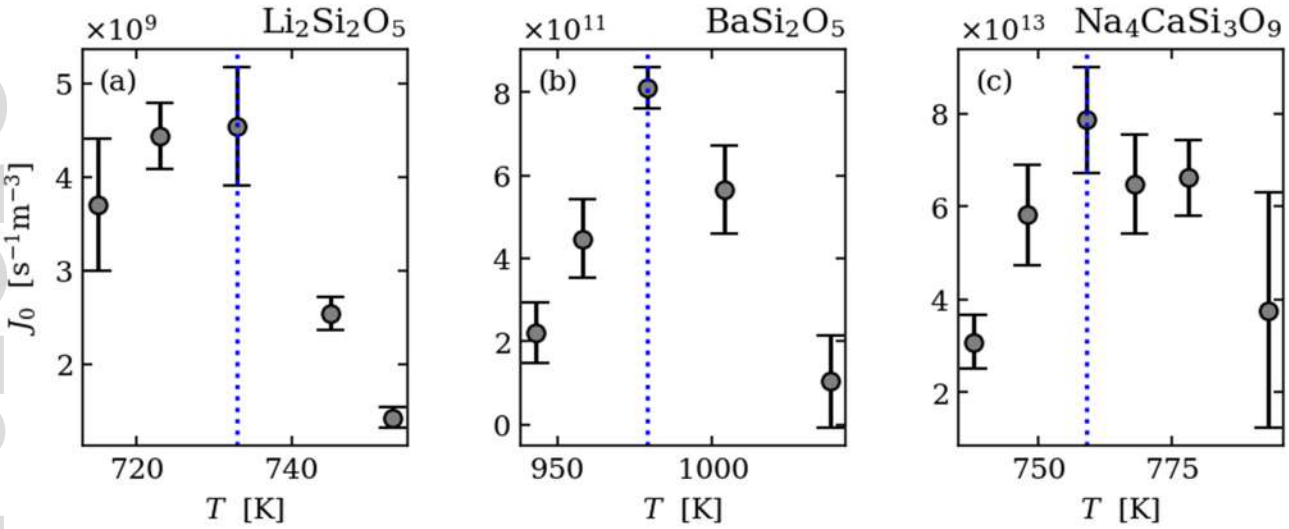

jace_17852_f5.tif

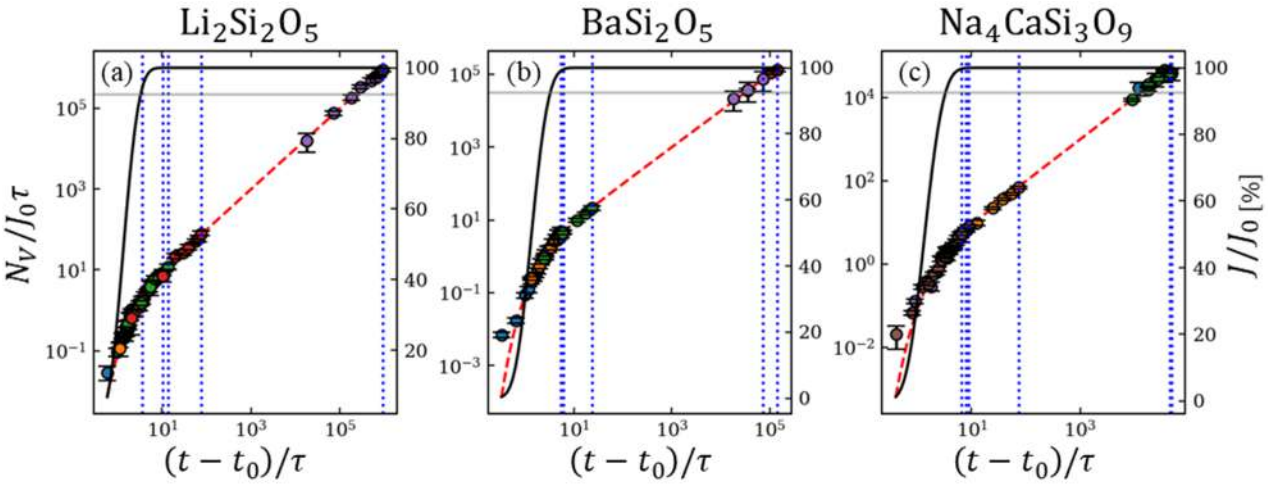

jace_17852_f6.tif

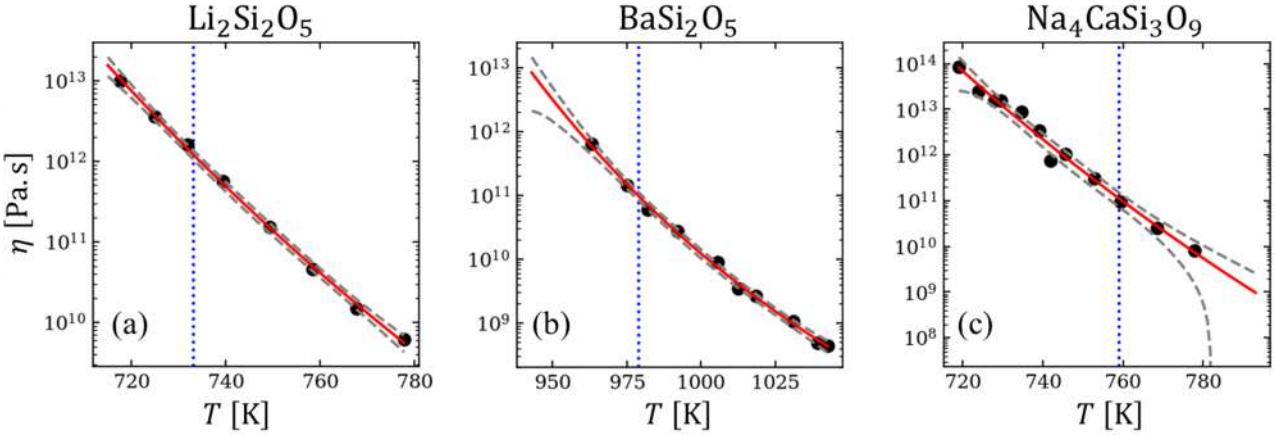

jace_17852_f7.tif

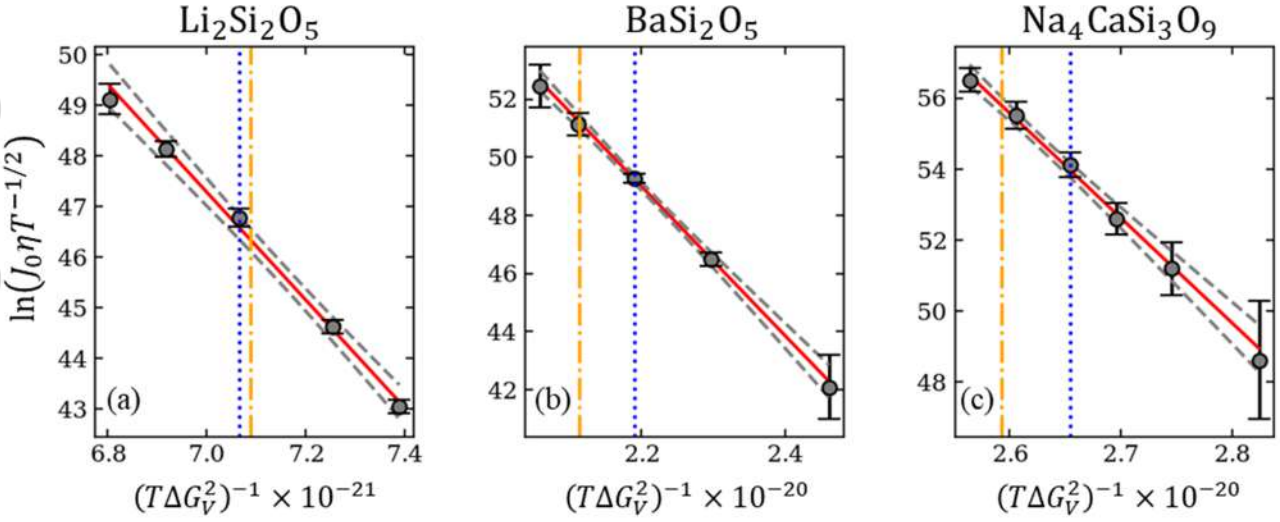

jace_17852_f8.tif

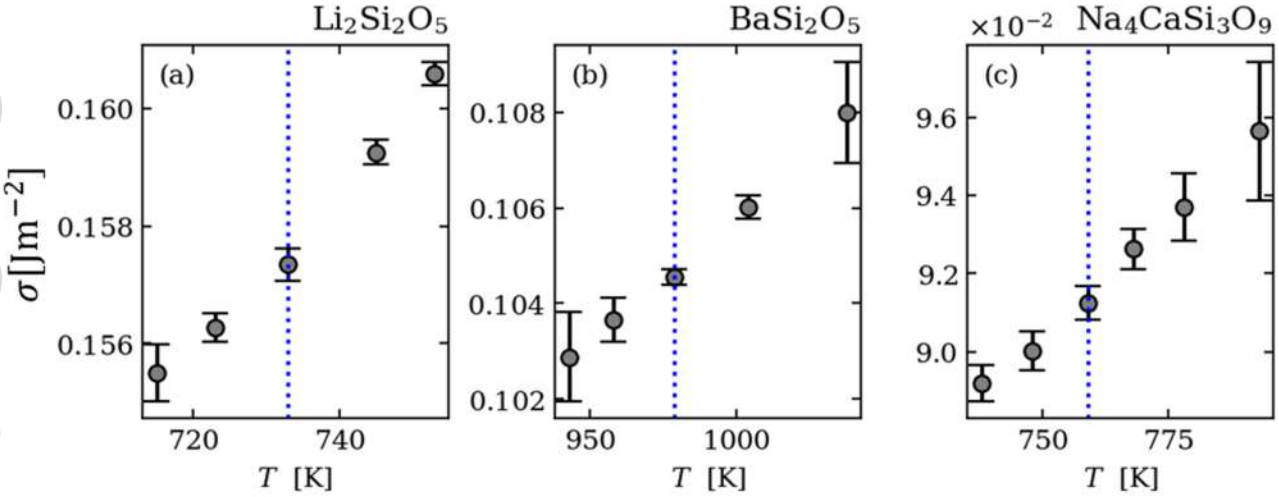

jace_17852_f9.tif